Developmental Cell
Article

Distinct Chemokine Signaling Regulates Integrin Ligand Specificity to Dictate Tissue-Specific Lymphocyte Homing

Hao Sun,[1,2] Jie Liu,[1,2] YaJuan Zheng,[1] YouDong Pan,[1] Kun Zhang,[1] and JianFeng Chen[1,*]
[1]State Key Laboratory of Cell Biology, Institute of Biochemistry and Cell Biology, Shanghai Institutes for Biological Sciences, Chinese Academy of Sciences, Shanghai 200031, China
[2]Co-first author
*Correspondence: jfchen@sibcb.ac.cn
http://dx.doi.org/10.1016/j.devcel.2014.05.002

SUMMARY

Immune surveillance and host defense depend on the precisely regulated trafficking of lymphocytes. Integrin $\alpha_4\beta_7$ mediates lymphocyte homing to the gut through its interaction with mucosal vascular address in cell adhesion molecule-1 (MAdCAM-1). $\alpha_4\beta_7$ also binds vascular cell adhesion molecule-1 (VCAM-1), which is expressed in other tissues. To maintain the tissue specificity of lymphocyte homing, $\alpha_4\beta_7$ must distinguish one ligand from the other. Here, we demonstrate that $\alpha_4\beta_7$ is activated by different chemokines in a ligand-specific manner. CCL25 stimulation promotes $\alpha_4\beta_7$-mediated lymphocyte adhesion to MAdCAM-1 but suppresses adhesion to VCAM-1, whereas CXCL10 stimulation has the opposite effect. Using separate pathways, CCL25 and CXCL10 stimulate differential phosphorylation states of the β_7 tail and distinct talin and kindlin-3 binding patterns, resulting in different binding affinities of MAdCAM-1 and VCAM-1 to $\alpha_4\beta_7$. Thus, our findings provide a mechanism for lymphocyte traffic control through the unique ligand-specific regulation of integrin adhesion by different chemokines.

INTRODUCTION

The control of systemic immune responses depends on the precisely regulated trafficking of lymphocytes from blood into different tissues (Butcher and Picker, 1996). The exquisite specificity of tissue-specific lymphocyte homing is mediated by the tightly controlled adhesion of lymphocytes to the vascular endothelium at target sites (Kunkel and Butcher, 2002). Lymphocytes express unique patterns of homing molecules, and the vascular endothelia in different tissues express the specific ligands (Mora and von Andrian, 2006). The interactions between homing molecules and their ligands enable lymphocytes to target to different tissues through a multistep process governed by selectins, integrins, and chemoattractants (Hartmann et al., 2008). Lymphocytes initially tether and roll on the endothelium by transiently interacting with endothelial cells via selectins and some integrins. Then integrins on lymphocytes become activated by chemoattractants presented on the endothelium, which is a key step in the recruitment of specific lymphocytes from blood to target tissues. Chemokines activate integrins through rapidly triggering an inside-out signaling that regulates the binding of intracellular effector proteins (e.g., talin and kindlin) to integrin cytoplasmic domains (Kinashi, 2005), which induces the conversion of inactive integrin in a bent conformation into its active form with an extended structure (Takagi et al., 2002).

Most integrins expressed on lymphocytes recognize multiple ligands (Humphries et al., 2006). Integrin $\alpha_4\beta_7$ is a homing receptor that targets lymphocytes in the bloodstream to mucosal tissues, especially the gut (Cox et al., 2010). The primary ligand for $\alpha_4\beta_7$ is mucosal vascular address in cell adhesion molecule-1 (MAdCAM-1), which is specifically expressed on the endothelium of high endothelial venules in the gut and gut-associated lymphoid tissues, such as Peyer's patches and mesenteric lymph nodes (mLNs; Berlin et al., 1995). Another ligand for $\alpha_4\beta_7$, vascular cell adhesion molecule-1 (VCAM-1), is widely expressed on stimulated endothelial cells of blood vessels, peripheral lymph nodes (pLNs), and bone marrow (Berlin-Rufenach et al., 1999). Theoretically, the ability of $\alpha_4\beta_7$ to bind multiple ligands should hinder the selectivity of lymphocyte trafficking to different tissues that express MAdCAM-1 or VCAM-1. Interestingly, lymphocytes activated in the gut have a propensity to home back to the intestine where MAdCAM-1 is expressed but are less likely to home to tissues expressing VCAM-1 (Johansson-Lindbom and Agace, 2007). However, the mechanism by which integrin $\alpha_4\beta_7$ selects between different binding ligands is unknown.

Herein, we demonstrate that integrin $\alpha_4\beta_7$ can be activated by distinct chemokines in a ligand-specific manner to mediate selective adhesion of lymphocytes to either MAdCAM-1 or VCAM-1. Via distinct pathways, CCL25 and CXCL10 stimulate different dephosphorylation of the β_7 tails, which lead to distinct binding patterns of talin and kindlin-3 to the β_7 tail that induce different activated forms of $\alpha_4\beta_7$ to mediate lymphocyte adhesion to either MAdCAM-1 or VCAM-1. Our findings provide a mechanism for lymphocyte traffic control through the ligand-specific regulation of integrin adhesion by different chemokines under certain circumstance.

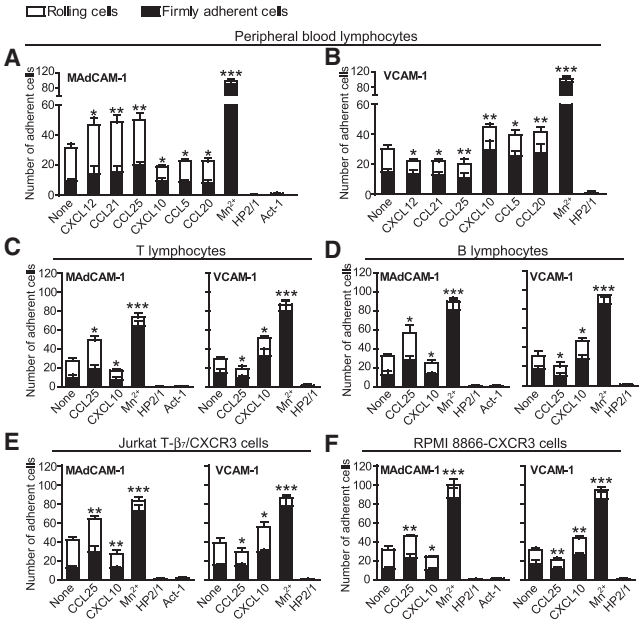

Figure 1. Chemokines Regulate Integrin $\alpha_4\beta_7$-Mediated Lymphocyte Adhesion to Different Ligands under Flow Conditions

(A and B) Adhesion of human PBLs to MAdCAM-1 (A) and VCAM-1 (B) at 1 dyn/cm^2 before and after chemokine stimulation. Cells were preincubated with 20 μg/ml AIIB2 to block $\alpha_4\beta_1$, and then infused into the flow chamber; 1 μg/ml Act-1 was used to block $\alpha_4\beta_7$-MAdCAM-1 interaction; 2 μg/ml HP2/1 was used to block the function of α_4 integrin; 0.5 mM Mn^{2+} was used as a control for integrin activation.

(C–F) Adhesion of T lymphocytes (C), B lymphocytes (D), Jurkat T-β_7/CXCR3 cells (E), and RPMI 8866-CXCR3 cells (F) to MAdCAM-1 and VCAM-1 at 1 dyn/cm^2 before and after chemokine stimulation. T lymphocytes, B lymphocytes, and Jurkat T-β_7/CXCR3 cells were preincubated with 20 μg/ml AIIB2 to block $\alpha_4\beta_1$, and then infused into the flow chamber.

Data represent the mean ± SD (n = 3). *p < 0.05, **p < 0.01, ***p < 0.001, NS, not significant (two-tailed Student's t test; asterisk indicates the changes of total adherent cells). See also Figure S1 and Movie S1.

RESULTS

Integrin $\alpha_4\beta_7$-Mediated Lymphocyte Adhesion to Different Ligands Is Regulated by Distinct Chemokines in a Ligand-Specific Manner

Chemokines have been shown to promote lymphocyte adhesion to the endothelium by activating integrins (De Smedt et al., 2001). To investigate the effect of different chemokines on integrin $\alpha_4\beta_7$-mediated lymphocyte adhesion to MAdCAM-1 and VCAM-1 under flow conditions, we first studied the adhesion of human peripheral blood lymphocytes (PBLs) on both substrates at a wall shear stress of 1 dyn/cm^2 in response to chemokine stimulation using a parallel wall flow chamber as described in the Experimental Procedures (Figures 1A and 1B; Movie S1 available online). A variety of lymphocyte-attracting chemokines (Campbell et al., 1998), including CXCL10, CXCL12, CCL5, CCL20, CCL21, and CCL25, were tested. Because PBLs express both $\alpha_4\beta_7$ and $\alpha_4\beta_1$ (Figure S1A), $\alpha_4\beta_1$-VCAM-1 interaction was disrupted by pretreating the cells with 20 μg/ml β_1 blocking antibody AIIB2 (Gui et al., 1996), which could efficiently block the adhesion of $\alpha_4\beta_1$-expressing Jurkat T cells to VCAM-1 (Figure S1B). Compared with the adhesion of PBLs to MAdCAM-1 and VCAM-1 before stimulation, activation of $\alpha_4\beta_7$ with 0.5 mM Mn^{2+} greatly increased the number of PBLs that adhered to both ligands. Strikingly, stimulation of PBLs with CXCL12, CCL21, and CCL25 significantly increased PBL adhesion to MAdCAM-1 but suppressed cell adhesion to VCAM-1. Conversely, CXCL10, CCL5, and CCL20 increased cell adhesion to VCAM-1 but suppressed cell adhesion to MAdCAM-1. Act-1, an antibody that specifically blocks human $\alpha_4\beta_7$-MAdCAM-1 interaction (Soler et al., 2009), completely abolished PBL adhesion to MAdCAM-1. In addition, cells treated with human α_4 blocking antibody HP2/1 did not adhere to both substrates (Erle et al., 1994; Kamata et al., 1995). Similar results were obtained when AIIB2-pretreated mouse splenic lymphocytes (SPLs) were examined (Figure S1C). Either blocking α_4 function by antibody PS/2 or using β_7-deficient SPLs abolished cell adhesion to both ligands, suggesting the adhesion of SPLs is $\alpha_4\beta_7$-specific. Considering that lymphocyte adhesion was most affected by CCL25 and CXCL10, we chose them as representatives of the two groups of chemokines. PBLs that were stimulated with soluble CCL25 and CXCL10 showed adhesive behaviors similar to those observed with immobilized chemokines (Figure S1D). Similar PBL adhesion patterns on MAdCAM-1 and VCAM-1 substrates were observed in the absence of $\alpha_4\beta_1$ blockade (Figure S1E). Collectively, the data demonstrate that activation of $\alpha_4\beta_7$ by different chemokines results in selective adhesion of lymphocytes to either MAdCAM-1 or VCAM-1.

Approximately 94% of PBLs are T and B lymphocytes (Figure S1A), and these cells may have different responses to chemokine stimulation. Therefore, we isolated T and B lymphocytes from PBLs (Figure S1A) and examined cell adhesion to MAdCAM-1 or VCAM-1 in flow in response to chemokine stimulation (Figures 1C and 1D). Both T and B lymphocytes showed adhesion behaviors similar to those of PBLs, indicating that the chemokine-induced selective adhesion of lymphocytes to MAdCAM-1 or VCAM-1 was not cell type dependent. To further confirm that the chemokine-induced differential cell adhesion to MAdCAM-1 or VCAM-1 was not due to the heterogeneity of PBLs, we established human T cell line Jurkat T-β_7/CXCR3 and B cell line RPMI 8866-CXCR3, which stably express $\alpha_4\beta_7$, CCR9 (CCL25 receptor), and CXCR3 (CXCL10 receptor) at a homogeneous level (Figure S1A), and examined the effects of CCL25 and CXCL10 on cell adhesion to MAdCAM-1 and VCAM-1 in flow (Figures 1E and 1F). Both Jurkat T-β_7/CXCR3 and RPMI 8866-CXCR3 cells showed adhesion behaviors similar to those of human T/B lymphocytes and PBLs in response to CCL25 and CXCL10 stimulations, indicating that CCL25 and CXCL10 induced differential adhesion of same type of cells to MAdCAM-1 or VCAM-1.

Ligand-Specific Activation of Integrin $\alpha_4\beta_7$ Depends on Distinct Chemokine Signaling

To investigate whether the ligand-specific activation of $\alpha_4\beta_7$ by different chemokines is due to the activation of distinct signaling pathways, a series of kinase inhibitors was screened, and two differential pathways that are related to the ligand-specific activation of $\alpha_4\beta_7$ by CCL25 and CXCL10 were identified (Figure 2A; Figure S2A). Inhibition of either PKCα/βI or p38α/β MAPK by their

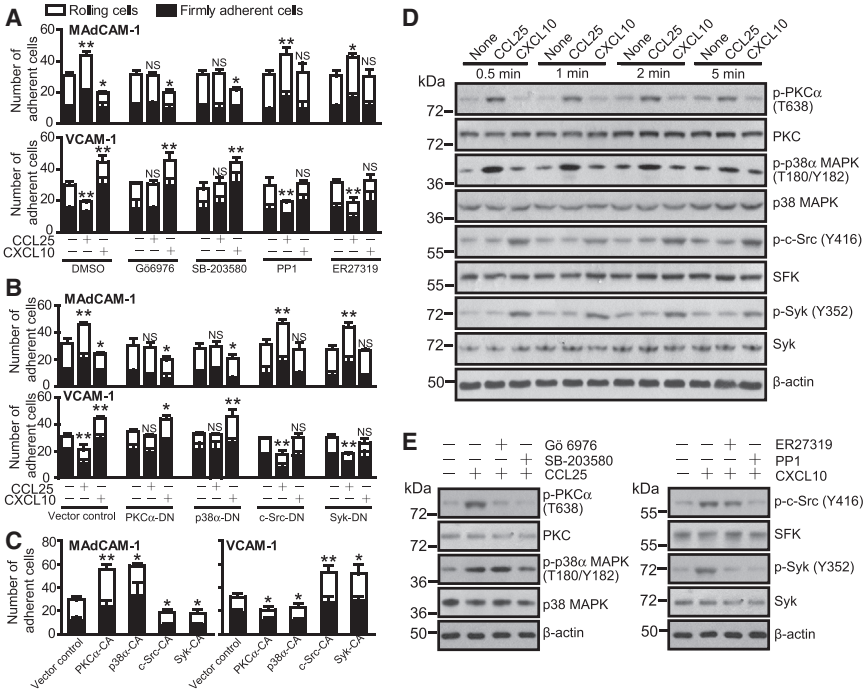

Figure 2. Ligand-Specific Activation of Integrin $\alpha_4\beta_7$ Depends on Distinct Signaling Pathways Triggered by Different Chemokines

(A) Effects of kinase inhibitors on chemokine-induced adhesion of RPMI 8866-CXCR3 cells to MAdCAM-1 and VCAM-1 at 1 dyn/cm^2.

(B) Effect of dominant-negative kinase mutant on chemokine-induced cell adhesion to MAdCAM-1 and VCAM-1 at 1 dyn/cm^2. RPMI 8866-CXCR3 cells transiently expressing each mutant were used.

(C) Effect of constitutively active kinase mutant on cell adhesion to MAdCAM-1 and VCAM-1 at 1 dyn/cm^2. RPMI 8866-CXCR3 cells transiently expressing each mutant were examined.

(D) Kinase activation over a 5 min after chemokine stimulation. The phosphorylation of PKCα, p38α MAPK, c-Src, and Syk from RPMI 8866-CXCR3 cells was determined by immunoblot analysis.

(E) Effects of kinase inhibitors on chemokine-induced kinase activation in RPMI 8866-CXCR3 cells.

Data in (A)–(C) represent the mean ± SD (n = 3). *p < 0.05, **p < 0.01, NS, not significant (two-tailed Student's t test; asterisk indicates the changes of total adherent cells). See also Figure S2.

specific inhibitors, Gö 6976 or SB-203580, specifically prevented CCL25-induced changes of adhesion of RPMI 8866-CXCR3 cells (Figure 2A) and PBLs (Figure S2A) to MAdCAM-1 and VCAM-1, indicating that PKCα/βI and p38α/β MAPK are essential to the ligand-specific regulation of $\alpha_4\beta_7$-mediated lymphocyte adhesion by CCL25. In addition, changes of cell adhesion to MAdCAM-1 and VCAM-1 after CXCL10 stimulation were inhibited by treatment with Src family kinase (SFK) inhibitor, PP1, or Syk inhibitor, ER27319, demonstrating an essential role of SFK and Syk in the ligand-specific regulation of $\alpha_4\beta_7$-mediated lymphocyte adhesion by CXCL10.

To confirm the roles of these kinases in the ligand-specific activation of $\alpha_4\beta_7$ by chemokines, dominant negative and constitutively active mutants of each kinase were transiently transfected into RPMI 8866-CXCR3 cells (Figures S2B and S2C). Overexpression of the dominant-negative mutant of PKCα (PKCα-DN), p38α MAPK (p38α-DN), c-Src (c-Src-DN), or Syk (Syk-DN) showed the same effect on cell adhesion to MAdCAM-1 and VCAM-1 as did the specific kinase inhibitors (Figure 2B). In contrast, overexpression of the dominant-negative mutant of PKCβI (PKCβI-DN), p38β MAPK (p38β-DN), or the other three members of SFK (Lck [Lck-DN], Fyn [Fyn-DN], or Hck [Hck-DN]) hardly affected the chemokine-stimulated cell adhesion to both ligands (Figure S2D). In addition, cells with overexpression of the constitutively active form of PKCα (PKCα-CA) or p38α MAPK (p38α-CA) showed similar adhesion to MAdCAM-1 and VCAM-1 as cells stimulated with CCL25, whereas overexpression of the constitutively active form of c-Src (c-Src-CA) or Syk (Syk-CA) showed the same effect of CXCL10 stimulation on cell adhesion to both ligands (Figure 2C). Thus, PKCα/p38α MAPK and c-Src/Syk are involved in the stimulation of differential cell adhesion to MAdCAM-1 and VCAM-1 by CCL25 and CXCL10, respectively.

To further confirm that CCL25 and CXCL10 induced activation of the kinases that were identified above, kinase phosphorylation in response to stimulation with soluble chemokines was compared over 5 min in RPMI 8866-CXCR3 cells (Figure 2D) and PBLs (Figure S2E). To exclude influence of ligand-binding induced integrin outside-in signaling, no integrin ligand was included in the chemokine-stimulation system. As expected, CCL25 stimulation specifically increased PKCα and p38α MAPK phosphorylation, but did not increase c-Src or Syk phosphorylation. On the contrary, CXCL10 stimulation increased c-Src and Syk phosphorylation, but did not increase PKCα or p38α MAPK phosphorylation. Inhibition of p38α MAPK by SB-203580 inhibited the CCL25-stimulated phosphorylation of both p38α MAPK and PKCα (Figure 2E; Figure S2F). In contrast, inhibition of PKCα by Gö 6976 inhibited the phosphorylation of PKCα, but not p38α MAPK. The data suggest that PKCα is located downstream of p38α MAPK. Inhibition of c-Src by PP1 inhibited the CXCL10-stimulated activation of both c-Src and Syk (Figure 2E; Figure S2F). However, the Syk inhibitor, ER27319, only inhibited Syk activation. These data suggest that Syk is located downstream of c-Src.

Collectively, the results demonstrate that CCL25 promotes $\alpha_4\beta_7$-mediated cell adhesion to MAdCAM-1 and suppresses adhesion to VCAM-1 through activation of the p38α MAPK/PKCα pathway. CXCL10 stimulates the opposite effect by activating the c-Src/Syk axis.

Different Chemokine Signaling Pathways Lead to Distinct Binding Patterns of Talin and Kindlin-3 to the β_7 Tail

The activation of GPCR signaling by chemokines regulates the binding of intracellular effector proteins to integrin tails, which triggers integrin's activation through inside-out signaling (Hogg et al., 2011). To investigate the effect of chemokine signaling on the

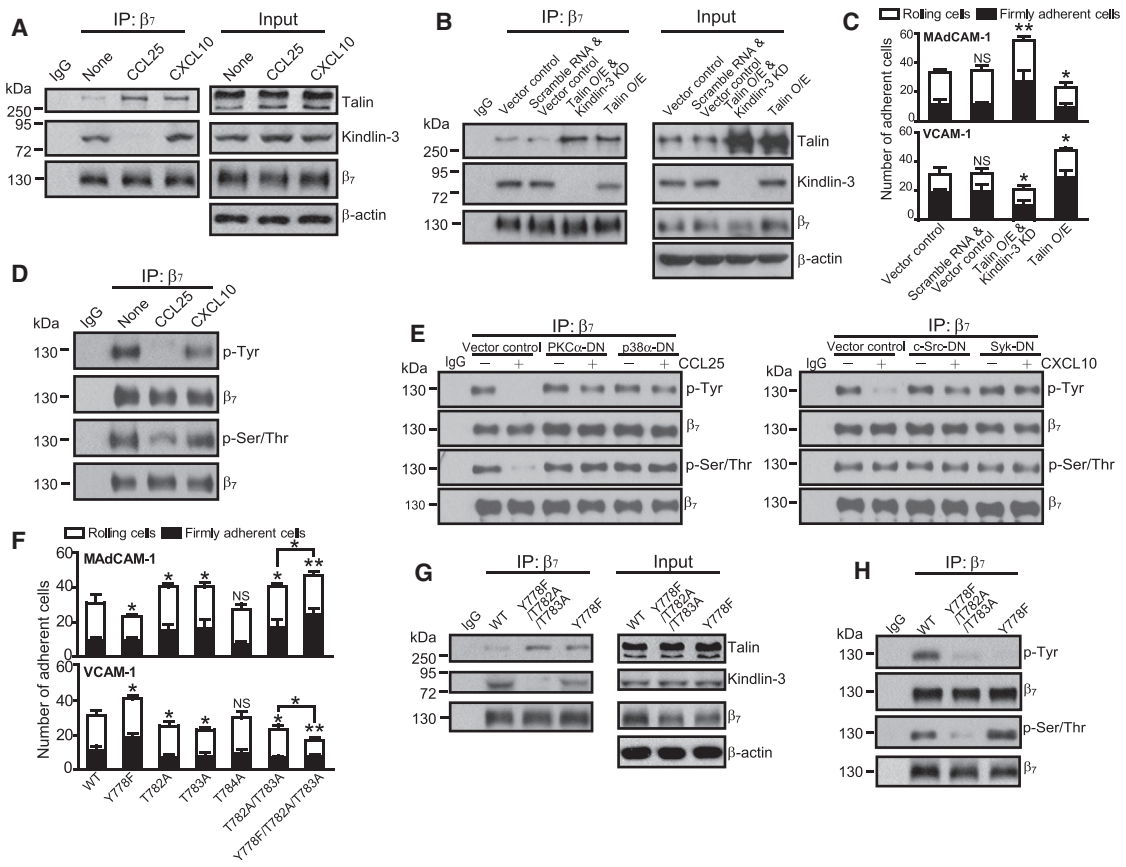

Figure 3. Different Chemokines Induce Distinct Integrin β_7 Tail Phosphorylation and Talin/Kindlin-3 Binding

(A and B) Coimmunoprecipitation of talin/kindlin-3 with β_7 from RPMI 8866-CXCR3 cells before and after chemokine stimulation (A) or with modified talin/kindlin-3 expression, including talin overexpression (Talin O/E) and talin overexpression combined with kindlin-3 knockdown (Talin O/E and Kindlin-3 KD; B).

(C) Effect of Talin O/E or Talin O/E and Kindlin-3 KD on RPMI 8866-CXCR3 cell adhesion to MAdCAM-1 and VCAM-1 at 1 dyn/cm^2.

(D) Tyr and Ser/Thr phosphorylation of β_7 in RPMI 8866-CXCR3 cells before and after chemokine stimulation.

(E) Effects of dominant-negative kinase mutant on Tyr and Ser/Thr phosphorylation of β_7 in RPMI 8866-CXCR3 cells before and after chemokine stimulation.

(F) Adhesion of Jurkat T cells expressing WT and mutant human β_7 to MAdCAM-1 and VCAM-1 at 1 dyn/cm^2. Cells were preincubated with 20 μg/ml AIIB2, and then infused into the flow chamber.

(G) Coimmunoprecipitation of talin/kindlin-3 with β_7 from Jurkat T cells expressing WT and mutant human β_7.

(H) Tyr and Ser/Thr phosphorylation of β_7 in Jurkat T cells expressing WT and mutant human β_7.

Data in (C) and (F) represent the mean ± SD (n = 3). *p < 0.05, **p < 0.01, NS, not significant (two-tailed Student's t test; asterisk indicates the changes of total adherent cells). See also Figure S3.

binding of effector proteins to $\alpha_4\beta_7$, we examined talin and kindlin, the major effector proteins that bind to the integrin β tails to regulate integrin activation (Moser et al., 2009). Kindlin-3 was selected from the three members of the kindlin family because it is expressed in cells of hematopoietic origin (Moser et al., 2008). The binding of talin and kindlin-3 to $\alpha_4\beta_7$ was determined by coimmunoprecipitation of these two proteins with $\alpha_4\beta_7$ in RPMI 8866-CXCR3 cells. Interestingly, CCL25 and CXCL10 stimulated different patterns of interaction between the β_7 tail and talin or kindlin-3 (Figure 3A). CCL25 stimulation markedly increased talin binding to $\alpha_4\beta_7$ but dramatically reduced kindlin-3 binding compared with nonstimulated cells. However, CXCL10 stimulation increased talin binding but hardly changed kindlin-3 binding. The data suggest that the intracellular signaling pathways that are activated by CCL25 and CXCL10 induce distinct binding patterns of talin and kindlin-3 to $\alpha_4\beta_7$, which may result in differential integrin activation. To test this hypothesis, we overexpressed talin to increase talin binding to the β_7 tail, which mimicked the CXCL10-induced talin/kindlin-3 binding pattern (Figure 3B). Additionally, talin overexpression combined with kindlin-3 knockdown mimicked the CCL25-induced talin/kindlin-3 binding pattern (Figure 3B). As expected, cells that overexpressed talin showed similar adhesion patterns on MAdCAM-1 and VCAM-1 substrates as cells that were stimulated with CXCL10 (Figure 3C). Cells that overexpressed talin and had kindlin-3 knocked down showed similar adhesion patterns as cells that were stimulated with CCL25 (Figure 3C).

Different Chemokines Induce Distinct Phosphorylation States of the β_7 Tail

The binding of talin and kindlin to integrins is regulated by integrin β tail phosphorylation. Talin binds the NPxY motif on the β tail to activate integrins, and phosphorylation of the Tyr in this motif inhibits talin binding (Sakai et al., 2001). Kindlin binds the distal

NxxY motif on the β tail to activate integrins (Legate and Fässler, 2009). Phosphorylation of an Ser/Thr-rich region between the NPxY/NxxY motifs is important for integrin to bind kindlin (Moser et al., 2008). To investigate whether phosphorylation of the NPxY and Ser/Thr-rich motifs in the β_7 tail is regulated by different chemokines, we compared Tyr and Ser/Thr phosphorylation in the β_7 tail in response to chemokine stimulations. CCL25 stimulation dramatically decreased the phosphorylation of Tyr and Ser/Thr residues in β_7, whereas CXCL10 stimulation only lowered the Tyr phosphorylation (Figure 3D). The results are consistent with the differential binding of talin and kindlin-3 to the β_7 tail in response to chemokine stimulations. In addition, overexpression of dominant negative mutant PKCα (PKCα-DN) or p38α MAPK (p38α-DN) inhibited the downregulation of Tyr and Ser/Thr phosphorylation in β_7 by CCL25 (Figure 3E), and overexpression of dominant-negative mutant c-Src (c-Src-DN) and Syk (Syk-DN) prevented the decrease of Tyr phosphorylation in β_7 upon CXCL10 stimulation (Figure 3E), indicating that the CCL25- and CXCL10-induced distinct phosphorylation states of β_7 are dependent on the activation of p38α MAPK/PKCα and c-Src/Syk pathways, respectively.

Next, we mutated Tyr778 in NPxY motif and Thr782-784 in the Ser/Thr-rich region on the β_7 tail, and stably expressed WT or mutant $\alpha_4\beta_7$ in Jurkat T cells (Figure S3A), which lack endogenous β_7. Y778F mutation was made to abolish phosphorylation of the Tyr in NPxY motif, which is expected to increase talin binding to the β_7 tail. As expected, Y778F showed similar effect of CXCL10 stimulation on cell adhesion to MAdCAM-1 and VCAM-1, suggesting Y778 dephosphorylation is important for the regulation by CXCL10 (Figure 3F). Mutation of the Ser/Thr-rich region to Ala (T782A, T783A, T784A) is expected to interrupt kindlin-3 binding to integrin β tails (Moser et al., 2008). Except for T784A, T782A, T783A, and T782A/T783A double mutation showed a similar effect of CCL25 stimulation on cell adhesion to both ligands, suggesting the dephosphorylation of T782 and T783 is important for regulation by CCL25 (Figure 3F). Notably, the addition of the Y778F mutation to T782A/T783A double mutation enhanced talin binding and decreased kindlin-3 binding to the β_7 tail (Figure 3G), which further enhanced the effect of T782A/T783A double mutation on the cell adhesion to both ligands (Figure 3F), suggesting the increased talin binding can enhance the effect of decreased kindlin-3 binding on cell adhesion. Thus, β_7 Y778F/T782A/T783A triple mutation or Y778F single mutation induced similar talin/kindlin-3 binding and cell adhesion that were stimulated by CCL25 or CXCL10, respectively (Figures 3F and 3G). Y778F/T782A/T783A triple mutation almost abolished the basal Tyr and Ser/Thr phosphorylation in β_7, suggesting the Tyr and Ser/Thr phosphorylation signals in β_7 are mainly from Y778 and T782/T783 (Figure 3H).

We next investigated whether the decreased phosphorylation of β_7 is due to the dephosphorylation of Tyr and Ser/Thr by phosphatases. It is reported that both PKC and Syk contribute to the activation of Tyr phosphatase Cdc25 (Hirano et al., 2000; Yu et al., 2004). In addition, PKC also contributes to the activation of Ser/Thr phosphatase PP2B (LaFayette et al., 2010). Our data showed that blocking either PP2B or Cdc25 with their specific inhibitors, Cypermethrin or NSC-663284, inhibited the CCL25-induced Ser/Thr or Tyr dephosphorylation of β_7 (Figure 4A) and diminished the changes of cell adhesion to MAdCAM-1 and VCAM-1 induced by CCL25 stimulation (Figure 4B). Moreover, inhibition of Cdc25 by NSC-663284 prevented the CXCL10-induced Tyr dephosphorylation in β_7 (Figure 4A) and the changes of cell adhesion induced by CXCL10 (Figure 4B). To further confirm the results, the dominant-negative mutants of PP2B and lymphocyte-expressing Cdc25 isoforms (Cdc25A and Cdc25C) were generated and then transiently transfected into cells (Figure S4A). Overexpression of the dominant-negative mutants of either PP2B (PP2B-DN) or Cdc25A (Cdc25A-DN), but not Cdc25C (Cdc25C-DN), prevented the changes of cell adhesion to both ligands induced by CCL25 (Figure 4C). Moreover, overexpression of Cdc25A-DN also inhibited the changes of cell adhesion induced by CXCL10. Consistently, coexpression of the active mutants of PP2B (PP2B-CA) and Cdc25A (Cdc25A-CA) showed the similar effect of CCL25 stimulation on cell adhesion to MAdCAM-1 and VCAM-1 (Figure 4D; Figure S4B). Overexpression of Cdc25A-CA alone showed a similar effect of CXCL10 stimulation on cell adhesion to both ligands. Collectively, these data demonstrate that CCL25-stimulated cell adhesion to MAdCAM-1 and VCAM-1 depends on both PP2B and Cdc25A, and CXCL10-induced cell adhesion only relies on Cdc25A. Thus, the chemokine-induced ligand-specific activation of $\alpha_4\beta_7$ depends on the differential dephosphorylation of Ser/Thr and Tyr in β_7 by PP2B and Cdc25A, respectively.

The chemokine-induced dephosphorylation of β_7 implies that β_7 integrin is phosphorylated at high stoichiometry in the resting state. Thus, we examined the stoichiometry of β_7 phosphorylation in nonstimulated RPMI 8866-CXCR3 cells (Ratnakumar et al., 2009). The results showed that approximately 40% or 50% of the cell surface β_7 integrins were Tyr or Ser/Thr phosphorylated before chemokine stimulation (Figures 4E and 4F). In addition, β_7 showed much higher level of Tyr and Ser/Thr phosphorylation than β_2 in resting state (Figures 4G and 4H). Thus, the data demonstrate that β_7 integrin is hyperphosphorylated in the nonstimulated state.

Distinct Chemokine Signaling Triggers Different MAdCAM-1 and VCAM-1 Binding to $\alpha_4\beta_7$

Next, we examined the binding of soluble MAdCAM-1 or VCAM-1 to $\alpha_4\beta_7$ in response to chemokine stimulation (Figure 5A). Compared with nonstimulated RPMI 8866-CXCR3 cells, CCL25 stimulation significantly increased MAdCAM-1 binding and decreased VCAM-1 binding. In contrast, CXCL10 stimulation showed opposite results. Treatment with Mn^{2+} maximally enhanced the binding of both ligands. Act-1 specifically blocked MAdCAM-1 binding. In addition, blocking α_4 by HP2/1 abolished binding of both ligands. These soluble ligand binding results are consistent with the results of cell adhesion in flow in response to chemokine stimulation. We next examined the effect of talin overexpression and kindlin-3 knockdown on soluble ligand binding to $\alpha_4\beta_7$ (Figure 5B). Consistently, cells that overexpressed talin, which mimicked the CXCL10-induced talin/kindlin-3 binding pattern, showed similar soluble ligand binding results as cells that were stimulated with CXCL10. In addition, cells that overexpressed talin and had kindlin-3 knocked down showed similar results as cells that were stimulated with CCL25.

Taken together, CCL25 and CXCL10 stimulate different binding patterns of talin and kindlin-3 to the β_7 tail, which induce differential binding of MAdCAM-1 and VCAM-1 to $\alpha_4\beta_7$.

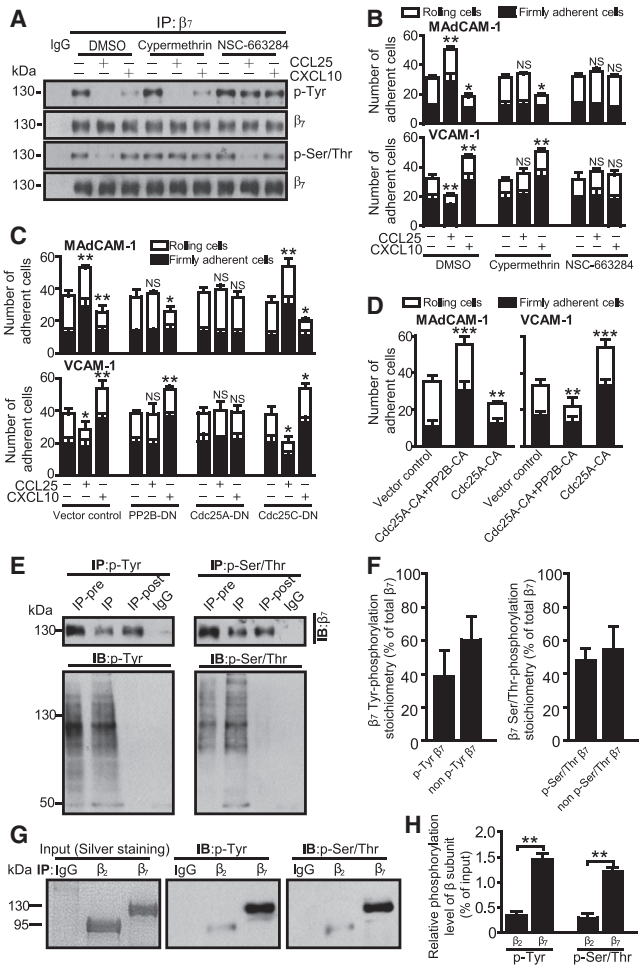

Figure 4. Chemokine-Induced Ligand-Specific Activation of $\alpha_4\beta_7$ Depends on the Dephosphorylation of the β_7 Tail by Phosphatases

(A) Effects of Ser/Thr and Tyr phosphatase inhibitors on β_7 phosphorylation in RPMI 8866-CXCR3 cells before and after chemokine stimulation.

(B) Effects of phosphatase inhibitors on the chemokine-induced adhesion of RPMI 8866-CXCR3 cells to MAdCAM-1 and VCAM-1 at 1 dyn/cm^2.

(C) Effects of dominant-negative PP2B, Cdc25A, and Cdc25C mutants on the chemokine-induced adhesion of RPMI 8866-CXCR3 cells to MAdCAM-1 and VCAM-1 at 1 dyn/cm^2.

(D) Effects of constitutively active PP2B and Cdc25A mutants on RPMI 8866-CXCR3 cell adhesion to MAdCAM-1 and VCAM-1 at 1 dyn/cm^2.

(E) The stoichiometry of β_7 phosphorylation. Tyr- or Ser/Thr-phosphorylated proteins from the membrane of nonstimulated RPMI 8866-CXCR3 cells were immunoprecipitated by anti-phosphotyrosine or anti-phosphoserine/threonine antibody. The same amount of the input (IP-pre), IP, and remaining lysate after IP (IP-post) were run on SDS-PAGE. β_7 integrins were blotted with monoclonal antibodies against human β_7. Tyr- or Ser/Thr-phosphorylated proteins were blotted as controls.

(F) Quantification of Tyr or Ser/Thr phosphorylation stoichiometry of β_7 according to (E).

(G) Phosphorylation levels of β_2 and β_7 in nonstimulated RPMI 8866-CXCR3 cells. β_2 and β_7 were immunoprecipitated from RPMI 8866-CXCR3 cells. The same amount of β_2 and β_7 was loaded on SDS-PAGE and confirmed by silver staining (Input). Tyr and Ser/Thr phosphorylation in β_2 and β_7 subunits were detected with immunoblot.

(H) Quantification of Tyr and Ser/Thr phosphorylation levels of β_2 and β_7 according to (G). The phosphorylation levels of β_2 and β_7 were normalized to the input.

Distinct Chemokine Signaling Stimulates $\alpha_4\beta_7$ to Regulate the Tissue Specificity of Lymphocyte Homing in Vivo

$\alpha_4\beta_7$ plays a critical role in tissue-specific lymphocyte homing to mLNs and pLNs, where MAdCAM-1 and VCAM-1 are highly expressed, respectively (Cording et al., 2014). Our study showed that CCL25 stimulation simultaneously enhanced the talin binding and reduced kindlin-3 binding to the β_7 tail, which increased the binding of $\alpha_4\beta_7$ to MAdCAM-1 and decreased $\alpha_4\beta_7$ binding to VCAM-1. In contrast, CXCL10 only enhanced talin binding to the β_7 tail, which induced opposite cell adhesion to both ligands. Thus, talin overexpression combined with kindlin-3 knockdown should promote lymphocyte homing to mLNs and inhibit lymphocyte homing to pLNs, whereas talin overexpression alone should have opposite effect. We then modified talin and kindlin-3 expression accordingly in SPLs and studied the effect on lymphocyte homing to mLNs and pLNs in mice. SPLs with talin overexpression alone (Talin O/E-SPLs) or simultaneous knockdown of kindlin-3 (Talin O/E and Kindlin-3 KD-SPLs; Figure S6A) were labeled with CFSE. SPLs that were transfected with vector alone (Vector control-SPLs) or along with scramble shRNA (Scramble RNA and Vector control-SPLs) were labeled with DID as a control. Equal numbers of CFSE-SPLs and DID-SPLs were mixed and then intravenously injected into C57BL/6J mice. Lymphoid organs were isolated 30 min after injection. The number of CFSE- or DID-labeled lymphocytes in mLNs and pLNs was determined with flow cytometry (Table S1), and then the homing index was determined (Figures 6A and 6B). Compared with Scramble RNA and Vector control-SPLs, Talin O/E and Kindlin-3 KD-SPLs homed significantly more to mLNs but less to pLNs (Figure 6A). In contrast, talin overexpression alone decreased SPL homing to mLNs but enhanced SPL homing to pLNs (Figure 6A). β_7-deficient Talin O/E and Kindlin-3 KD-SPLs and Talin O/E-SPLs showed no preference for homing to pLNs and mLNs (Figure 6B), indicating that the distinct homing specificities are β_7-dependent. In addition, the effects of different talin/kindlin expression on the adhesion of WT and β_7-deficient SPLs to MAdCAM-1 and VCAM-1 in flow were examined (Figure S6B). The in vitro cell adhesion results are consistent with the in vivo data. Thus, these data demonstrate that CCL25- and CXCL10-induced differential talin/kindlin-3 binding to the β_7 tail regulates the specificity of lymphocyte homing to tissues that express MAdCAM-1 or VCAM-1 in vivo.

Next, we investigated whether the ligand-specific activation of $\alpha_4\beta_7$ by CCL25 or CXCL10 regulates the tissue specificity of lymphocyte homing to mLNs and pLNs in mice. The competitive in vivo homing of CCL25 or CXCL10-stimulated SPLs versus nonstimulated SPLs was examined. Because the effects of CCL25 and CXCL10 on $\alpha_4\beta_7$-mediated adhesion of SPLs to both ligands can persist for at least 1 hr (Figure S6C), lymphoid organs were isolated 30 min after injection and the homing indices for different chemokine stimulations were then determined. Compared with the nonstimulated SPLs, CCL25 stimulation significantly increased SPL homing to mLNs, but decreased

Data represent the mean ± SD (n = 3). *p < 0.05, **p < 0.01, ***p < 0.001, NS, not significant (two-tailed Student's t test; asterisk in B–D indicates the changes of total adherent cells). See also Figure S4.

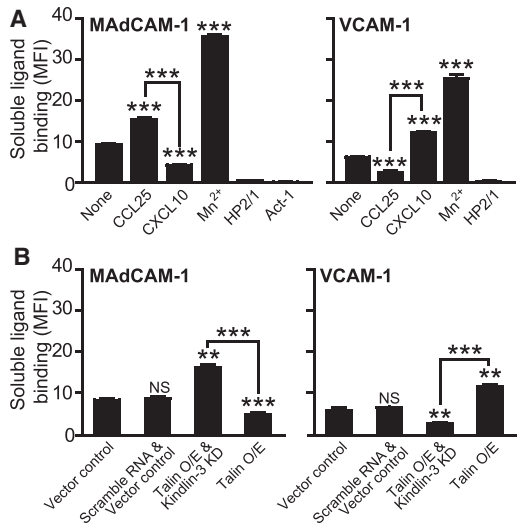

Figure 5. Chemokines Induce Different Affinities of Integrin $\alpha_4\beta_7$

(A and B) Binding of soluble MAdCAM-1 and VCAM-1 to RPMI 8866-CXCR3 cells before and after chemokine stimulation (A) or with modified talin/kindlin-3 expression (B); 0.5 mM Mn^{2+} was used as a control for integrin activation; 1 μg/ml Act-1 and 2 μg/ml HP2/1 were used to block the human $\alpha_4\beta_7$-MAdCAM-1 interaction and the function of α_4 integrin, respectively.

Data represent the mean ± SD (n = 3). **p < 0.01, ***p < 0.001, NS, not significant (two-tailed Student's t test). See also Figure S5.

cell homing to pLNs (Figure 6C). In contrast, CXCL10 treatment decreased SPL homing to mLNs but enhanced SPL homing to pLNs (Figure 6C). β_7-deficient SPLs did not show any preference for homing to mLNs or pLNs after chemokine stimulation (Figure 6D), indicating that the increased homing specificity of lymphocytes to mLNs and pLNs by CCL25 or CXCL10 stimulation is $\alpha_4\beta_7$-dependent. In addition, inhibition of either PKCα or p38α MAPK abolished the CCL25-induced change of SPL homing to mLNs and pLNs (Figures 6E and 6F). And inhibition of c-Src or Syk specifically abolished the effects of CXCL10 stimulation on SPL homing to mLNs and pLNs (Figures 6G and 6H). Thus, CCL25 and CXCL10 regulate the tissue specificity of lymphocyte homing to mLNs and pLNs in vivo, which are dependent on p38α MAPK/PKCα and c-Src/Syk signaling pathways, respectively.

To confirm that the chemokine-induced $\alpha_4\beta_7$ ligand specificity switch is deployed in vivo to alter lymphocyte homing in a physiologically significant manner, we investigated the lymphocyte homing to mLNs and pLNs in mice following viral infection, which has been shown to induce *CXCL10* expression (Borgland et al., 2000). Wild-type, β_7-deficient and CXCR3-deficient mice were intravenously injected with adenovirus, and *CXCL10* expression was significantly increased in mLNs and pLNs at transcription level 6 hr after virus injection compared with PBS-injected control mice (Figure S6D). Then, pLNs and mLNs were isolated and the number of lymphocytes was determined (Figure S6E). Compared with PBS control mice, the number of lymphocytes significantly increased in pLNs but decreased in mLNs in viral infection mice. In contrast, the number of lymphocytes in mLNs and pLNs showed no significant change in β_7-deficient or CXCR3-deficient mice after viral infection. Thus, viral infection-induced *CXCL10* expression promotes lymphocyte homing to pLNs but suppresses lymphocyte homing to mLNs in vivo, which is β_7- and CXCR3-dependent. Next, we examined the homing of lymphocytes to pLNs and mLNs in viral infection mice and PBS control mice. Compared with PBS control mice, the number of wild-type (WT) SPLs significantly increased in pLNs, but decreased in mLNs in viral infection mice (Figures S6F and S6G). However, there was no difference in homing of β_7-deficient or CXCR3-deficient SPLs to pLNs and mLNs between viral infection and PBS control mice (Figures S6F and S6G), indicating the effect of CXCL10 on lymphocyte homing to pLNs and mLNs is β_7- and CXCR3-dependent. Collectively, viral infection-induced *CXCL10* expression enhances lymphocyte homing to pLNs, but suppresses lymphocyte homing to mLNs in mice, suggesting that CXCL10 regulates lymphocyte homing to distinct tissues in vivo by switching the ligand specificity of $\alpha_4\beta_7$.

DISCUSSION

Our study demonstrates the switch of integrin ligand-specificity by distinct chemokine signaling and its underlying molecular mechanism. These findings reveal a potential mechanism for maintaining the specificity of lymphocyte homing to different tissues through the ligand-specific activation of integrins by different chemokines (Figure 6; Figure S6), which could be an important complement to the current model of lymphocyte tissue-specific homing.

In addition to $\alpha_4\beta_7$, lymphocytes also express $\alpha_4\beta_1$, which binds VCAM-1 and contributes to lymphocyte homing to pLNs (Santamaria Babi et al., 1995). Thus, we investigated the effects of CCL25 and CXCL10 on cell adhesion to MAdCAM-1 and VCAM-1 without blocking $\alpha_4\beta_1$ (Figure S1E). Consistent with the fact that $\alpha_4\beta_1$ only binds VCAM-1, we did observe an increase of adherent PBLs to immobilized VCAM-1 (Figure S1E) compared with the cells that $\alpha_4\beta_1$ function was blocked (Figure 1B). Notably, the CCL25- and CXCL10-induced distinct cell adhesion to VCAM-1 remained before and after blocking $\alpha_4\beta_1$. Furthermore, we examined the effects of CCL25 and CXCL10 stimulations on SPL homing to pLNs and mLNs with (Figure S6H) or without blocking $\alpha_4\beta_1$ (Figures 6C and 6D). Consistent with the fact that VCAM-1 highly expressed in pLNs but not in mLNs (Mori et al., 1999), blocking $\alpha_4\beta_1$ decreased the number of SPLs that homed to pLNs, but hardly affected cell homing to mLN (Table S1). The CCL25 and CXCL10 stimulation-induced distinct homing patterns of SPLs to pLNs and mLNs were unchanged before and after blocking $\alpha_4\beta_1$ (Figure S6H). Taken together, $\alpha_4\beta_1$ only contributes to the homing of lymphocytes to VCAM-1-expressing pLNs, but not MAdCAM-1-expressing mLNs. The presence of $\alpha_4\beta_1$ could increase the total number of cells homed to pLNs, but did not change the CCL25- and CXCL10-induced distinct adhesion patterns that depend on the function of $\alpha_4\beta_7$. We also examined $\alpha_4\beta_1$-mediated cell adhesion to VCAM-1 in responses to different chemokines using β_7-deficient SPLs (Figure S1F). Unlike suppressing the $\alpha_4\beta_7$-medaited cell adhesion to VCAM-1, CXCL12, CCL21, or CCL25 stimulation did not change $\alpha_4\beta_1$-mediated cell adhesion to VCAM-1. CXCL10, CCL20, or CCL5 stimulation increased cell adhesion to VCAM-1, which was

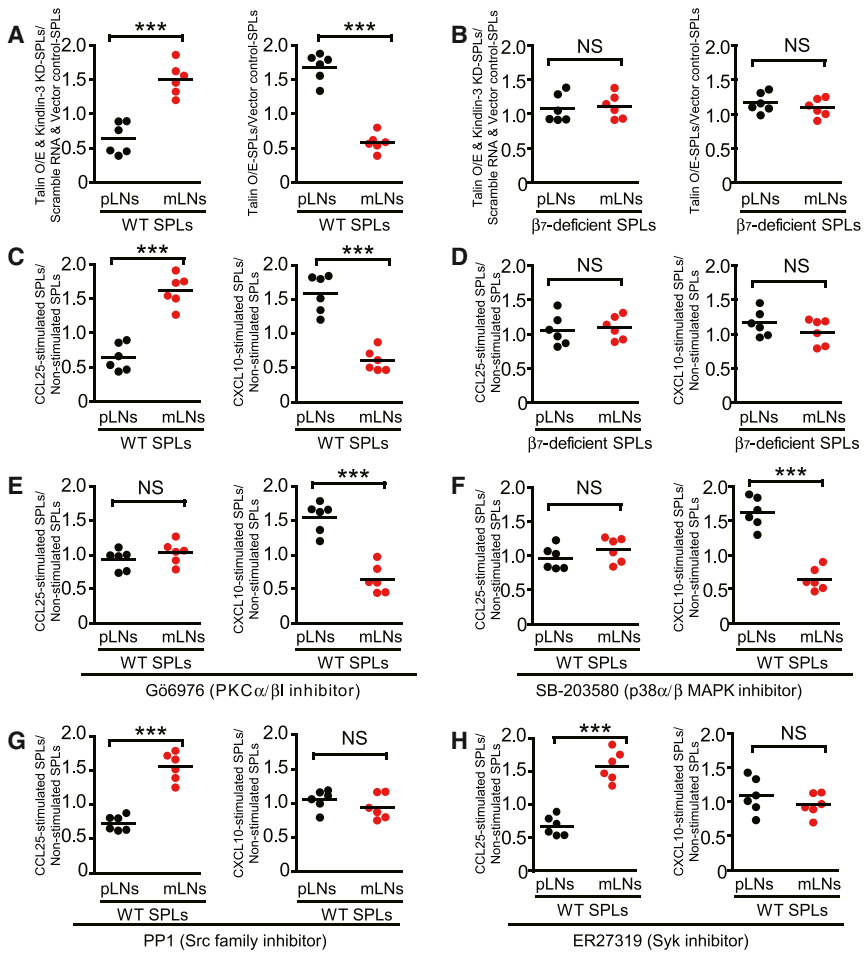

Figure 6. Different Chemokine Signaling Regulates Tissue-Specific Homing of Lymphocytes

(A and B) In vivo competitive homing of WT SPLs (A) or β_7-deficient SPLs (B) with talin overexpression combined with kindlin-3 knockdown (Talin O/E and Kindlin-3 KD-SPLs) or talin overexpression alone (Talin O/E-SPLs). The ratios of Talin O/E and Kindlin-3 KD-SPLs over Scramble RNA and Vector control-SPLs or Talin O/E-SPLs over Vector control-SPLs that homed to pLNs and mLNs in C57BL/6J mice are shown.

(C and D) In vivo competitive homing of WT SPLs (C) or β_7-deficient SPLs (D) before and after chemokine stimulation. The ratio of chemokine-simulated SPLs over nonsimulated SPLs that homed to pLNs and mLNs in C57BL/6J mice is shown.

(E–H) Effect of kinase inhibitor on tissue-specific homing of lymphocytes in mice before and after chemokine stimulation. WT SPLs were pretreated with Gö6976 (E), SB-203580 (F), PP1 (G), or ER27319 (H) before chemokine stimulation. The ratio of chemokine-simulated SPLs over nonsimulated SPLs that homed to pLNs and mLNs in C57BL/6J mice is shown.

Data represent the mean (n = 6). ***$p < 0.001$, NS, not significant (two-tailed Student's t test). See also Figure S6 and Table S1.

similar to the effect of these chemokines on $\alpha_4\beta_7$-medaited cell adhesion.

Our data showed that CXCL12, CCL21, or CCL25 promoted lymphocyte adhesion to MAdCAM-1 but suppressed cell adhesion to VCAM-1. In contrast, CXCL10, CCL5, or CCL20 showed an opposite effect on lymphocyte adhesion to both ligands. CCL25, CXCL12, or CCL21 specifically increased the phosphorylation of PKCα and p38α MAPK, whereas CXCL10, CCL20, or CCL5 specifically increased the phosphorylation of c-Src and Syk (Figure 2D; Figures S2E and S2G). Thus, the two groups of chemokines activated the p38α MAPK/PKCα and c-Src/Syk pathways respectively, which differentially activated $\alpha_4\beta_7$ and resulted in different binding affinity to MAdCAM-1 and VCAM-1.

As a control for the opposite regulatory effects of CCL25 and CXCL10, stimulation of cells with CCL25 and CXCL10 at the same time did not change cell adhesion to MAdCAM-1 and VCAM-1 when compared with nonstimulated cells (Figure S1G). The data suggest that costimulation by CCL25 and CXCL10 leads to the counteraction of opposite regulatory effects of CCL25 and CXCL10. Thus, the net regulatory effect on cell adhesion is compromised in comparison with the results of cells stimulated by individual chemokine.

Filamin has been shown to compete with talin for binding to integrin β tails (Kiema et al., 2006). However, simultaneous increase of filamin and talin binding to the β_7 tail was observed after overexpression of dominant active RSK2 (Gawecka et al., 2012), suggesting that both filamin and talin can associate with the β_7 tail without competition under certain conditions. Previous studies have shown that binding of filamin to integrin is inhibited by the phosphorylation of the Ser/Thr-rich region in the β tail (Legate and Fässler, 2009). Because kindlin binding to integrin depends on the phosphorylation of this Ser/Thr-rich region, kindlin might compete with filamin for binding to integrin β tails. Here, we monitored filamin binding to β_7 in response to chemokine stimulation (Figures S3B and S3C). CXCL10 stimulation simultaneously increased talin binding and reduced filamin A binding to $\alpha_4\beta_7$, but hardly affected kindlin-3 binding, suggesting filamin A might compete with talin for binding to β_7 under the conditions induced by CXCL10. Interestingly, CCL25 stimulation markedly increased both the binding of filamin A and talin, but dramatically reduced kindlin-3 binding to $\alpha_4\beta_7$, suggesting a potential competition between filamin A and kindlin-3 for binding to β_7 under the CCL25-induced condition. Thus, our data suggest that filamin can compete with either kindlin-3 or talin for binding to β_7 tail under different circumstances.

Kindlin-3 is believed to be essential for the activation of β_1 and β_3 integrins (Lefort and Ley, 2012; Moser et al., 2008). Knockdown of kindlin-3 is sufficient to block the β_2-mediated cell adhesion to ICAM-1 (Figures S3D–S3F). Additionally, the requirement of kindlin-3 for integrin $\alpha_L\beta_2$ and $\alpha_4\beta_1$ to bind ligands is only critical when integrin ligand level is low, but of less importance when integrin ligand level is high (Moretti et al., 2013), suggesting that kindlin-3 has distinct regulatory functions under different conditions. Interestingly, this study has shown that talin binding alone

compared to both talin and kindlin-3 binding to integrin tails has different effects on $\alpha_L\beta_2$ conformation (Lefort et al., 2012), which is consistent with our finding that distinct talin and kindlin-3 binding patterns induce differential activation of $\alpha_4\beta_7$ and result in different binding of MAdCAM-1 and VCAM-1 to $\alpha_4\beta_7$.

Integrin affinity and valency are both important for integrin-mediated cell adhesion. Therefore, we examined $\alpha_4\beta_7$ subcellular distribution in response to chemokine stimulation (Figure S5). Compared with no discernable clustering of $\alpha_4\beta_7$ on nonstimulated PBLs, obvious clusters of $\alpha_4\beta_7$ were induced by antibody crosslinking (Kim et al., 2004). CCL25 and CXCL10 induced similar weak clustering of $\alpha_4\beta_7$ on the surface of PBLs. Thus, CCL25 and CXCL10 do not induce different subcellular distribution of $\alpha_4\beta_7$.

Leukocyte adhesion deficiency (LAD) is a very rare genetic disorder that affects the body's immune system. The hallmarks of LAD are defects in the leukocyte adhesion process, marked leukocytosis, and recurrent infections (Akbari and Zadeh, 2001). Among the three general genotypes of LAD, LAD-III is due to the mutation in the *kindlin3* gene (Svensson et al., 2009). The kindlin-3 mutation leads to the deficiency of its binding to integrin. Clinical cases showed that some patients with LAD exhibited certain signs and symptoms suggestive of a Crohn's disease-like disorder (D'Agata et al., 1996), suggesting the aberrant lymphocytes accumulate in the gut in particular cases of LAD (possible LAD-III). These data are consistent with our findings that decreased kindlin-3 binding together with increased talin binding to the β_7 tail enhanced lymphocyte adhesion to MAdCAM-1 and homing to the gut.

EXPERIMENTAL PROCEDURES

Flow Chamber Assay

A polystyrene Petri dish was coated with 20 μl of MAdCAM-1/Fc (10 μg/ml) or VCAM-1/Fc (10 μg/ml) alone or with chemokines (2 μg/ml) in coating buffer (PBS, 10 mM $NaHCO_3$, pH 9.0) for 1 hr at 37°C followed by blocking with 2% BSA in coating buffer for 1 hr at 37°C. Cells were diluted to 1×10^6 cells/ml in HBSS (10mM HEPES, 1 mM Ca^{2+}/Mg^{2+}) and immediately perfused through the flow chamber at a constant flow of 1 dyn/cm^2. For the soluble chemokine stimulation, cells were prestimulated for the indicated times with soluble chemokines (0.5 μg/ml) at room temperature before being perfused into the flow chamber. For the kinase or phosphatase inhibition, cells were pretreated with 1 μM Gö6976 for 1 hr at 37°C; or 10 μM SB-203580, 10 μM PP1, or 10 μM ER27319 for 30 min at 37°C, respectively.

All adhesive interactions between the flowing cells and the coated substrates were determined by manually tracking the motions of individual cells for 1 min as previously described (Ebisuno et al., 2010). The motion of each adherent cell was monitored for 10 s following the initial adhesion point, and two categories of cell adhesion were defined. Adhesion was defined as rolling adhesion if the adherent cells were followed by rolling motions $\geq$ 5 s with a velocity of at least 1 μm/s (for PBLs and SPLs) or 2 μm/s (for Jurkat T-β_7/CXCR3 and RPMI 8866-CXCR3 cells due to the larger cell size), whereas a firmly adherent cell was defined as a cell that remained adherent and stationary for at least 10 s.

In Vivo Competitive Lymphocyte Homing

SPLs were isolated from WT mice (C57BL/6J mice, from SLAC) or β_7-deficient mice (*Itgb7*$^{-/-}$ C57BL/6J mice, from Jackson Laboratory). In Figures 6A and 6B, Talin O/E and Kindlin-3 KD SPLs (or Talin O/E SPLs) and Scramble RNA and Vector control SPLs (or Vector control SPLs) were labeled with CFSE and DID, respectively. In Figures 6C–6H, chemokine-stimulated SPLs and nonstimulated SPLs were labeled with CFSE and DID, respectively. Equal numbers (1×10^7) of CFSE- or DID-labeled cells are mixed and injected intravenously into recipient mice via the tail vein. After 30 min, the recipient mice were killed, and lymphocytes from pLNs and mLNs were harvested. The absolute cell numbers were determined by flow cytometry (FACS Calibur, BD), and the ratios of CFSE- and DID-labeled cells in pLNs or mLNs were calculated. In Figures 6E–6H, SPLs were pretreated with kinase inhibitors, then stimulated with chemokines.

Animals

The WT C57BL/6J mice were obtained from SLAC. The β_7- deficient (*Itgb7*$^{-/-}$) and CXCR3-deficient (*Cxcr3*$^{-/-}$) C57BL/6J mice were obtained from the Jackson Laboratory. The genotype of knockout mice was verified with PCR amplification (Taq DNA Polymerase, Vazyme). All experimental animal procedures were approved by the Institutional Animal Care and Research Advisory Committee of the Institute of Biochemistry and Cell Biology, Shanghai Institutes for Biological Sciences, Chinese Academy of Sciences.

Statistical Analysis

Statistical significance was determined by two-tailed Student's t test using PRISM software (version 5.00, GraphPad Software). The resulting p values are indicated as follows: NS, $p > 0.05$; *, $0.01 < p < 0.05$; **, $0.001 < p < 0.01$; ***, $p < 0.001$. Data represent the mean ± SD of at least three independent experiments. Western blot results showed the representative images from three independent experiments.

SUPPLEMENTAL INFORMATION

Supplemental Information includes Supplemental Experimental Information, six figures, one table, and one movie and can be found with this article online at http://dx.doi.org/10.1016/j.devcel.2014.05.002.

AUTHOR CONTRIBUTIONS

H.S., J.L., and J.F.C. designed experiments; H.S., J.L., Y.J.Z., Y.D.P., and K.Z. performed experiments and analyzed data; H.S., J.L., and J.F.C. interpreted results; and the manuscript was drafted by H.S. and J.L. and edited by J.F.C.

ACKNOWLEDGMENTS

We thank the Chemical Biology Core Facility of SIBCB for compound library support and Dr. JunLin Guan, DianQing (Dan) Wu, DangSheng Li, and GaoXiang Ge for advice on experiments. This work was supported by grants from the National Basic Research Program of China (2010CB529703, 2014CB541905), National Natural Science Foundation of China (31190061, 31271487), and Science and Technology Commission of Shanghai Municipality (11JC1414200) to J.F.C. and grants from the National Natural Science Foundation of China (31301150), China Postdoctoral Science Foundation (2012M520954), and Postdoctoral Research Program from SIBS (2013KIP302) to H.S. The authors gratefully acknowledge the support of the SA-SIBS scholarship program.

Received: December 6, 2013
Revised: March 18, 2014
Accepted: April 30, 2014
Published: June 19, 2014

REFERENCES

Akbari, H., and Zadeh, M.M. (2001). Leukocyte adhesion deficiency. Indian J. Pediatr. *68*, 77–79.

Berlin, C., Bargatze, R.F., Campbell, J.J., von Andrian, U.H., Szabo, M.C., Hasslen, S.R., Nelson, R.D., Berg, E.L., Erlandsen, S.L., and Butcher, E.C. (1995). alpha 4 integrins mediate lymphocyte attachment and rolling under physiologic flow. Cell *80*, 413–422.

Berlin-Rufenach, C., Otto, F., Mathies, M., Westermann, J., Owen, M.J., Hamann, A., and Hogg, N. (1999). Lymphocyte migration in lymphocyte function-associated antigen (LFA)-1-deficient mice. J. Exp. Med. *189*, 1467–1478.

Borgland, S.L., Bowen, G.P., Wong, N.C., Libermann, T.A., and Muruve, D.A. (2000). Adenovirus vector-induced expression of the C-X-C chemokine IP-10 is mediated through capsid-dependent activation of NF-kappaB. J. Virol. *74*, 3941–3947.

Butcher, E.C., and Picker, L.J. (1996). Lymphocyte homing and homeostasis. Science *272*, 60–66.

Campbell, J.J., Hedrick, J., Zlotnik, A., Siani, M.A., Thompson, D.A., and Butcher, E.C. (1998). Chemokines and the arrest of lymphocytes rolling under flow conditions. Science *279*, 381–384.

Cording, S., Wahl, B., Kulkarni, D., Chopra, H., Pezoldt, J., Buettner, M., Dummer, A., Hadis, U., Heimesaat, M., Bereswill, S., et al. (2014). The intestinal micro-environment imprints stromal cells to promote efficient Treg induction in gut-draining lymph nodes. Mucosal Immunol. *7*, 359–368.

Cox, D., Brennan, M., and Moran, N. (2010). Integrins as therapeutic targets: lessons and opportunities. Nat. Rev. Drug Discov. *9*, 804–820.

D'Agata, I.D., Paradis, K., Chad, Z., Bonny, Y., and Seidman, E. (1996). Leucocyte adhesion deficiency presenting as a chronic ileocolitis. Gut *39*, 605–608.

De Smedt, T., Butz, E., Smith, J., Maldonado-López, R., Pajak, B., Moser, M., and Maliszewski, C. (2001). CD8alpha(-) and CD8alpha(+) subclasses of dendritic cells undergo phenotypic and functional maturation in vitro and in vivo. J. Leukoc. Biol. *69*, 951–958.

Ebisuno, Y., Katagiri, K., Katakai, T., Ueda, Y., Nemoto, T., Inada, H., Nabekura, J., Okada, T., Kannagi, R., Tanaka, T., et al. (2010). Rap1 controls lymphocyte adhesion cascade and interstitial migration within lymph nodes in RAPL-dependent and -independent manners. Blood *115*, 804–814.

Erle, D.J., Briskin, M.J., Butcher, E.C., Garcia-Pardo, A., Lazarovits, A.I., and Tidswell, M. (1994). Expression and function of the MAdCAM-1 receptor, integrin alpha 4 beta 7, on human leukocytes. J. Immunol. *153*, 517–528.

Gawecka, J.E., Young-Robbins, S.S., Sulzmaier, F.J., Caliva, M.J., Heikkilä, M.M., Matter, M.L., and Ramos, J.W. (2012). RSK2 protein suppresses integrin activation and fibronectin matrix assembly and promotes cell migration. J. Biol. Chem. *287*, 43424–43437.

Gui, G.P., Wells, C.A., Yeomans, P., Jordan, S.E., Vinson, G.P., and Carpenter, R. (1996). Integrin expression in breast cancer cytology: a novel predictor of axillary metastasis. Eur. J. Surg. Oncol. *22*, 254–258.

Hartmann, T.N., Grabovsky, V., Pasvolsky, R., Shulman, Z., Buss, E.C., Spiegel, A., Nagler, A., Lapidot, T., Thelen, M., and Alon, R. (2008). A crosstalk between intracellular CXCR7 and CXCR4 involved in rapid CXCL12-triggered integrin activation but not in chemokine-triggered motility of human T lymphocytes and CD34+ cells. J. Leukoc. Biol. *84*, 1130–1140.

Hirano, T., Ishihara, K., and Hibi, M. (2000). Roles of STAT3 in mediating the cell growth, differentiation and survival signals relayed through the IL-6 family of cytokine receptors. Oncogene *19*, 2548–2556.

Hogg, N., Patzak, I., and Willenbrock, F. (2011). The insider's guide to leukocyte integrin signalling and function. Nat. Rev. Immunol. *11*, 416–426.

Humphries, J.D., Byron, A., and Humphries, M.J. (2006). Integrin ligands at a glance. J. Cell Sci. *119*, 3901–3903.

Johansson-Lindbom, B., and Agace, W.W. (2007). Generation of gut-homing T cells and their localization to the small intestinal mucosa. Immunol. Rev. *215*, 226–242.

Kamata, T., Puzon, W., and Takada, Y. (1995). Identification of putative ligand-binding sites of the integrin alpha 4 beta 1 (VLA-4, CD49d/CD29). Biochem. J. *305*, 945–951.

Kiema, T., Lad, Y., Jiang, P., Oxley, C.L., Baldassarre, M., Wegener, K.L., Campbell, I.D., Ylänne, J., and Calderwood, D.A. (2006). The molecular basis of filamin binding to integrins and competition with talin. Mol. Cell *21*, 337–347.

Kim, M., Carman, C.V., Yang, W., Salas, A., and Springer, T.A. (2004). The primacy of affinity over clustering in regulation of adhesiveness of the integrin alphaLbeta2. J. Cell Biol. *167*, 1241–1253.

Kinashi, T. (2005). Intracellular signalling controlling integrin activation in lymphocytes. Nat. Rev. Immunol. *5*, 546–559.

Kunkel, E.J., and Butcher, E.C. (2002). Chemokines and the tissue-specific migration of lymphocytes. Immunity *16*, 1–4.

LaFayette, S.L., Collins, C., Zaas, A.K., Schell, W.A., Betancourt-Quiroz, M., Gunatilaka, A.A., Perfect, J.R., and Cowen, L.E. (2010). PKC signaling regulates drug resistance of the fungal pathogen Candida albicans via circuitry comprised of Mkc1, calcineurin, and Hsp90. PLoS Pathog. *6*, e1001069.

Lefort, C.T., and Ley, K. (2012). Neutrophil arrest by LFA-1 activation. Front. Immunol. *3*, 157.

Lefort, C.T., Rossaint, J., Moser, M., Petrich, B.G., Zarbock, A., Monkley, S.J., Critchley, D.R., Ginsberg, M.H., Fässler, R., and Ley, K. (2012). Distinct roles for talin-1 and kindlin-3 in LFA-1 extension and affinity regulation. Blood *119*, 4275–4282.

Legate, K.R., and Fässler, R. (2009). Mechanisms that regulate adaptor binding to beta-integrin cytoplasmic tails. J. Cell Sci. *122*, 187–198.

Mora, J.R., and von Andrian, U.H. (2006). T-cell homing specificity and plasticity: new concepts and future challenges. Trends Immunol. *27*, 235–243.

Moretti, F.A., Moser, M., Lyck, R., Abadier, M., Ruppert, R., Engelhardt, B., and Fässler, R. (2013). Kindlin-3 regulates integrin activation and adhesion reinforcement of effector T cells. Proc. Natl. Acad. Sci. USA *110*, 17005–17010.

Mori, N., Horie, Y., Gerritsen, M.E., Anderson, D.C., and Granger, D.N. (1999). Anti-inflammatory drugs and endothelial cell adhesion molecule expression in murine vascular beds. Gut *44*, 186–195.

Moser, M., Nieswandt, B., Ussar, S., Pozgajova, M., and Fässler, R. (2008). Kindlin-3 is essential for integrin activation and platelet aggregation. Nat. Med. *14*, 325–330.

Moser, M., Legate, K.R., Zent, R., and Fässler, R. (2009). The tail of integrins, talin, and kindlins. Science *324*, 895–899.

Ratnakumar, S., Kacherovsky, N., Arms, E., and Young, E.T. (2009). Snf1 controls the activity of adr1 through dephosphorylation of Ser230. Genetics *182*, 735–745.

Sakai, T., Jove, R., Fässler, R., and Mosher, D.F. (2001). Role of the cytoplasmic tyrosines of beta 1A integrins in transformation by v-src. Proc. Natl. Acad. Sci. USA *98*, 3808–3813.

Santamaria Babi, L.F., Moser, R., Perez Soler, M.T., Picker, L.J., Blaser, K., and Hauser, C. (1995). Migration of skin-homing T cells across cytokine-activated human endothelial cell layers involves interaction of the cutaneous lymphocyte-associated antigen (CLA), the very late antigen-4 (VLA-4), and the lymphocyte function-associated antigen-1 (LFA-1). J. Immunol. *154*, 1543–1550.

Soler, D., Chapman, T., Yang, L.L., Wyant, T., Egan, R., and Fedyk, E.R. (2009). The binding specificity and selective antagonism of vedolizumab, an anti-alpha4beta7 integrin therapeutic antibody in development for inflammatory bowel diseases. J. Pharmacol. Exp. Ther. *330*, 864–875.

Svensson, L., Howarth, K., McDowall, A., Patzak, I., Evans, R., Ussar, S., Moser, M., Metin, A., Fried, M., Tomlinson, I., and Hogg, N. (2009). Leukocyte adhesion deficiency-III is caused by mutations in KINDLIN3 affecting integrin activation. Nat. Med. *15*, 306–312.

Takagi, J., Petre, B.M., Walz, T., and Springer, T.A. (2002). Global conformational rearrangements in integrin extracellular domains in outside-in and inside-out signaling. Cell *110*, 599–11.

Yu, B.Z., Zheng, J., Yu, A.M., Shi, X.Y., Liu, Y., Wu, D.D., Fu, W., and Yang, J. (2004). Effects of protein kinase C on M-phase promoting factor in early development of fertilized mouse eggs. Cell Biochem. Funct. *22*, 291–298.